Expansions of adaptive-like NK cells with a tissue-resident phenotype in human lung and blood

Demi Brownlie[a,1], Marlena Scharenberg[a,1], Jeff E. Mold[b], Joanna Hård[b], Eliisa Kekäläinen[c,d,e], Marcus Buggert[a], Son Nguyen[f,g], Jennifer N. Wilson[a], Mamdoh Al-Ameri[h], Hans-Gustaf Ljunggren[a], Nicole Marquardt[a,2,3], and Jakob Michaëlsson[a,2]

[a]Center for Infectious Medicine, Department of Medicine Huddinge, Karolinska Institutet, 14152 Stockholm, Sweden; [b]Department of Cell and Molecular Biology, Karolinska Institutet, 171 77 Stockholm, Sweden; [c]Translational Immunology Research Program, University of Helsinki, 00014 Helsinki, Finland; [d]Department of Bacteriology and Immunology, University of Helsinki, 00014 Helsinki, Finland; [e]Helsinki University Central Hospital Laboratory, Division of Clinical Microbiology, Helsinki University Hospital, 00290 Helsinki, Finland; [f]Department of Microbiology, Perelman School of Medicine, University of Pennsylvania, Philadelphia, PA 19104; [g]Institute for Immunology, Perelman School of Medicine, University of Pennsylvania, Philadelphia, PA 19104; and [h]Thoracic Surgery, Department of Molecular Medicine and Surgery, Karolinska University Hospital, Karolinska Institutet, 171 76 Stockholm, Sweden

Human adaptive-like "memory" $CD56^{dim}CD16^+$ natural killer (NK) cells in peripheral blood from cytomegalovirus-seropositive individuals have been extensively investigated in recent years and are currently explored as a treatment strategy for hematological cancers. However, treatment of solid tumors remains limited due to insufficient NK cell tumor infiltration, and it is unknown whether large expansions of adaptive-like NK cells that are equipped for tissue residency and tumor homing exist in peripheral tissues. Here, we show that human lung and blood contains adaptive-like $CD56^{bright}CD16^-$ NK cells with hallmarks of tissue residency, including expression of CD49a. Expansions of adaptive-like lung tissue-resident NK (trNK) cells were found to be present independently of adaptive-like $CD56^{dim}CD16^+$ NK cells and to be hyperresponsive toward target cells. Together, our data demonstrate that phenotypically, functionally, and developmentally distinct subsets of adaptive-like NK cells exist in human lung and blood. Given their tissue-related character and hyperresponsiveness, human lung adaptive-like trNK cells might represent a suitable alternative for therapies targeting solid tumors.

NK cells | adaptive | memory | lung | tissue-resident

Natural killer (NK) cells are a crucial part of the innate immune system by eliminating virus-infected and malignant cells and boosting immunity through the production of proinflammatory cytokines including IFN-γ and TNF. The concept of adaptive-like or "memory" NK cells has emerged from studies in mice (1–4) and humans (5–10). Adaptive-like NK cells have a distinct phenotype and increased target cell responsiveness, as well as features of longevity and superior recall potential reminiscent of memory T cells (11).

Most studies of human adaptive-like NK cells have focused on subsets of $NKG2C^+(KIR^+)CD56^{dim}CD16^+$ NK cells found to be expanded and stably maintained in blood of ∼30 to 40% of human cytomegalovirus (HCMV)-seropositive individuals (5, 10). Adaptive-like $CD56^{dim}CD16^+$ NK cells in human peripheral blood (herein defined as adaptive-like $CD56^{dim}CD16^+$ peripheral blood NK [pbNK] cells) have a distinctive phenotypic (5, 10), epigenetic (8, 9), and functional (8–10) profile compared to conventional NK cells and have been suggested to contribute to immunity against HCMV (1, 12). Importantly, adaptive-like $CD56^{dim}CD16^+$ pbNK cells are currently explored for improving NK cell-mediated cancer therapies. While adoptive NK cell transfer showed optimistic results in the treatment of hematological malignancies, targeting solid tumors was less successful due to poor migration to and infiltration into the tumor (reviewed in ref. 13). In these cases, adaptive-like NK cells with an increased capacity to infiltrate tissues, e.g., through coexpression of tissue-specific ligands, might be desirable.

We and others recently identified a subset of tissue-resident $CD49a^+CD56^{bright}CD16^-$ NK cells in the human lung (14, 15). The human lung is a frequent site of infection with viruses such as influenza virus and HCMV, as well as a reservoir for latent HCMV (16). Although human $CD56^{dim}CD16^+$ lung NK cells are hyporesponsive to ex vivo target cell stimulation (17), exposure of human lung NK cells to virus-infected cells is likely to result in functional NK cell priming and expansion of distinct NK cell subsets. However, whether there are expansions of adaptive-like tissue-resident NK (trNK) cells in the human lung is to date unknown.

Here, we identify and examine a $CD49a^+KIR^+NKG2C^+$ $CD56^{bright}CD16^-$ NK cell population (herein defined as adaptive-like $CD49a^+$ NK cells) with features of tissue residency in human lung and blood, which is distinct from adaptive-like $CD56^{dim}CD16^+$ pbNK cells. In donors with expansions of adaptive-like $CD49a^+$ NK cells in the lung, a small but detectable population of adaptive-like $CD49a^+$ NK cells was observed in paired peripheral blood. While adaptive-like $CD56^{dim}CD16^+$ pbNK cells (as commonly identified in peripheral blood of HCMV-seropositive donors) and

Significance

Respiratory diseases are leading causes of death worldwide. However, the local immune cell composition in the human lung and individual outliers within the population still remain largely undescribed. We here identify adaptive-like NK cell expansions with tissue-resident traits in lung and blood in approximately 20% of individuals. This particular NK cell subset, which differed from adaptive-like $CD16^+$ blood NK cells, was hyperresponsive to target cell stimulation. Individuals with such in vivo-primed, expanded NK cells will likely experience a different course of acute lung disease such as viral infections. Furthermore, we believe that target cell-hyperresponsive tissue-resident NK cells represent a future tool in the treatment of lung cancer.

IMMUNOLOGY AND INFLAMMATION

adaptive-like CD49a$^+$ NK cells in lung and blood shared a common core gene signature, we identified several unique features of each population, indicating that they may represent developmentally distinct populations. Notably, NK cells from donors with an adaptive-like CD49a$^+$ NK cell expansion in the lung were hyperresponsive toward target cells. Thus, we provide evidence indicating that adaptive-like CD49a$^+$ NK cells in the human lung represent a population distinct from adaptive-like CD56^{dim}CD16$^+$ pbNK cells with potential implications in lung surveillance and future therapies against solid tumors.

Results

Adaptive-Like NK Cells Can Be Identified in Human Lung. We first set out to investigate whether expansions of adaptive-like KIR$^+$NKG2C$^+$ NK cells could be identified per se in the human lung. Circulating populations of adaptive-like CD56^{dim}CD16$^+$ NK cells could be identified in both the peripheral blood and lungs from patients undergoing surgery for suspected lung cancer (Fig. 1A). Surprisingly, KIR and NKG2C were also coexpressed on less differentiated CD56^{bright}CD16$^-$ lung NK cells, with varying frequencies between donors (Fig. 1 B and C; SI Appendix, Fig. S1A), shows the gating strategy to identify KIR$^+$NKG2C$^+$ CD56^{bright}CD16$^-$ and CD56^{dim}CD16$^+$ NK cells). In several donors, the frequencies of KIR$^+$NKG2C$^+$CD56^{bright}CD16$^-$ NK cells in human lung vastly exceeded those previously described for CD16$^-$ NK cells in the liver (7), with up to 98% of CD56^{bright}CD16$^-$ lung NK cells coexpressing KIR and NKG2C (Fig. 1 B and C).

Next, we assessed phenotypic features of KIR$^+$NKG2C$^+$ CD56^{bright}CD16$^-$ lung NK cells in an unbiased manner using high-dimensional flow cytometry. Uniform manifold approximation and expression (UMAP) analysis revealed a distinct subset of cells with an expression pattern consistent with adaptive-like NK cells found in peripheral blood and liver, including low expression of Siglec-7 and CD161 and high expression of NKG2C, KIRs, and CD2 (7, 8, 18) (Fig. 1D). Unlike adaptive-like CD56^{dim}CD16$^+$ pbNK cells, KIR$^+$NKG2C$^+$CD56^{bright}CD16$^-$ NK cells expressed lower levels of CD45RA and NKp80 and higher levels of CD8 (Fig. 1D). Manual analysis of individual samples confirmed lower expression of ILT2 and FcεR1γ as compared to KIR$^+$NKG2C$^+$CD56^{dim}CD16$^+$ lung NK cells (Fig. 1 E and F). Furthermore, KIR$^+$NKG2C$^+$CD56^{bright}CD16$^-$ lung NK cells displayed high expression of Eomes and NKG2A but similar levels in T-bet expression, revealing a phenotype distinct from human adaptive-like KIR$^+$NKG2C$^+$CD16$^-$ NK cells in the liver (7) (Fig. 1 E and F). Together, we here identify a previously uncharacterized population of an adaptive-like NK cell subset in the human lung, which is phenotypically distinct from adaptive-like CD56^{dim}CD16$^+$ pbNK cells.

Adaptive-Like CD56^{bright}CD16$^-$ NK Cells in Human Lung Have a Tissue-Resident Phenotype. Human lung trNK cells are characterized by expression of CD69 and the integrins CD49a and CD103 (14, 15). Strikingly, the vast majority of NKG2C$^+$CD56^{bright}CD16$^-$ NK cells identified by UMAP analysis coexpressed CD69 (80%) and CD49a (77%), and a substantial proportion (38%) also coexpressed CD103 (Fig. 2 A and B), suggesting tissue residency of adaptive-like CD56^{bright}CD16$^-$ NK cells in the lung. KIR$^+$NKG2C$^+$ NK cells coexpressing CD49a, CD69, or CD103 were mainly CD56^{bright}CD16$^-$ (Fig. 2 C and D), further demonstrating that they are clearly distinct from adaptive-like CD56^{dim}CD16$^+$ pbNK cells.

To further characterize adaptive-like CD49a$^+$ NK cells in the lung, we compared the gene expression profiles of sorted adaptive-like KIR$^+$NKG2C$^+$ lung trNK cells to nonadaptive KIR$^-$NKG2C$^-$ lung trNK and nontrNK cell subsets using RNA sequencing (RNA-seq; Fig. 2 E and F; sorting strategy shown in SI Appendix, Fig. S1 B and C). By principal component analysis (PCA), adaptive-like KIR$^+$NKG2C$^+$ trNK cells clustered

separately from all other NK cell subsets (Fig. 2E). A total of 102 differentially expressed genes (DEGs) were identified comparing adaptive-like KIR$^+$NKG2C$^+$ trNK cells and KIR$^-$NKG2C$^-$ trNK cells (adjusted P value [P$_{adj}$] < 0.05, log2 fold change [FC] > 1), including several KIR genes, CD8A, GPR183 (EBI2), IRF8, and SH2D1B (EAT2), and genes encoding for the transcription factors MafF (MAFF) and ZNF498 (ZSCAN25; Fig. 2F). GPR183 has been demonstrated to be crucial for tissue-specific migration of innate lymphoid cells (19), while EAT2 expression has previously been shown to be down-regulated in adaptive-like CD56^{dim}CD16$^+$ pbNK cells (8). Although up-regulation of both IRF8 and THEMIS2 has been reported to be essential for NK cell-mediated responses against MCMV infection (20, 21), the expression of both genes was low in adaptive-like CD49a$^+$ NK cells in human lung (Fig. 2F), indicating different activation pathways in adaptive-like NK cells in mice and humans. A number of shared DEGs were identified in adaptive-like lung trNK cells and in adaptive-like NKG2C$^+$CD57$^+$CD56^{dim}CD16$^+$ pbNK cells (Gene Expression Omnibus [GEO] accession GSE117614; ref. 22) compared to their non–adaptive-like counterparts, including higher expression of KLRC2 (NKG2C), KLRC3 (NKG2E), GZMH, ITGAD (CD11d), and RGS9 and lower expression of KLRB1 (CD161), KLRC1 (NKG2A), KLRF1 (NKp80), IL18RAP, and FCER1G (Fig. 2 F and G). These results demonstrate that adaptive-like CD49a$^+$ lung NK cells and adaptive-like CD56^{dim}CD16$^+$ pbNK cells share a common core gene set specific for adaptive-like NK cells.

Adaptive-like NK cells in peripheral blood and in the human liver commonly have a distinct KIR expression profile, which is dominated by KIRs that bind to self-HLA class I (self-KIRs) (7, 10, 23). In the lung, adaptive-like CD49a$^+$ NK cells displayed unique KIR expression patterns compared to CD16$^+$ NK cells in paired blood or lung (Fig. 2 H–J; SI Appendix, Figs. S2 and S1D, show the gating strategy). High expression of KIRs on adaptive-like CD49a$^+$ NK cells was limited to inhibitory self-KIRs (Fig. 2K). Notably, even in a donor with adaptive-like CD49$^+$ NK cells and adaptive-like CD56^{dim}CD16$^+$ NK cells, the KIR-expression profile differed between the two subsets (Fig. 2H and SI Appendix, Fig. S2). These results suggest a subset-specific development and/or differentiation of adaptive-like NK cells in blood and lung.

Together, adaptive-like CD49a$^+$ NK cells in the human lung express a unique profile of activating and inhibitory NK cell receptors (e.g., NKG2A, KIR, NKp80) as well as adaptor, signaling, and effector molecules (FcεR1γ, SH2D1B, granzyme H), identifying them as a bona fide adaptive-like NK cell subset distinct from previously described adaptive-like CD56^{dim}CD16$^+$ pbNK cells.

Lung Adaptive-Like trNK Cells Are Hyperresponsive to Target Cells. To determine whether adaptive-like CD49a$^+$ lung NK cells differed functionally from nonadaptive CD56^{bright}CD16$^-$ lung trNK cells, we first compared expression levels of genes associated with functional competence (Fig. 3A). Adaptive-like CD49a$^+$ lung NK cells expressed higher levels of IFNG, IL32, XCL1, and GZMH and lower levels of GNLY, GZMA, GZMK, IL2RB, and IL18RAP compared to nonadaptive lung trNK cells (Fig. 3A). Expression levels of PRF1 and GZMB did not differ between adaptive- and nonadaptive-like CD49a$^+$ NK cells (Fig. 3A). However, ex vivo protein expression was increased for granzyme B in adaptive-like CD49a$^+$ NK cells (Fig. 3 B and C). NK cells from donors with an expansion of adaptive-like CD49a$^+$ NK cells in the lung degranulated stronger and produced more TNF compared to those from donors without such expansions (Fig. 3D). In particular, NK cells coexpressing CD49a and KIR degranulated strongly and produced high levels of TNF and IFN-γ upon target cell stimulation (Fig. 3 D–F and SI Appendix, Fig. S3). The hyperresponsiveness of adaptive-like CD49a$^+$ lung NK
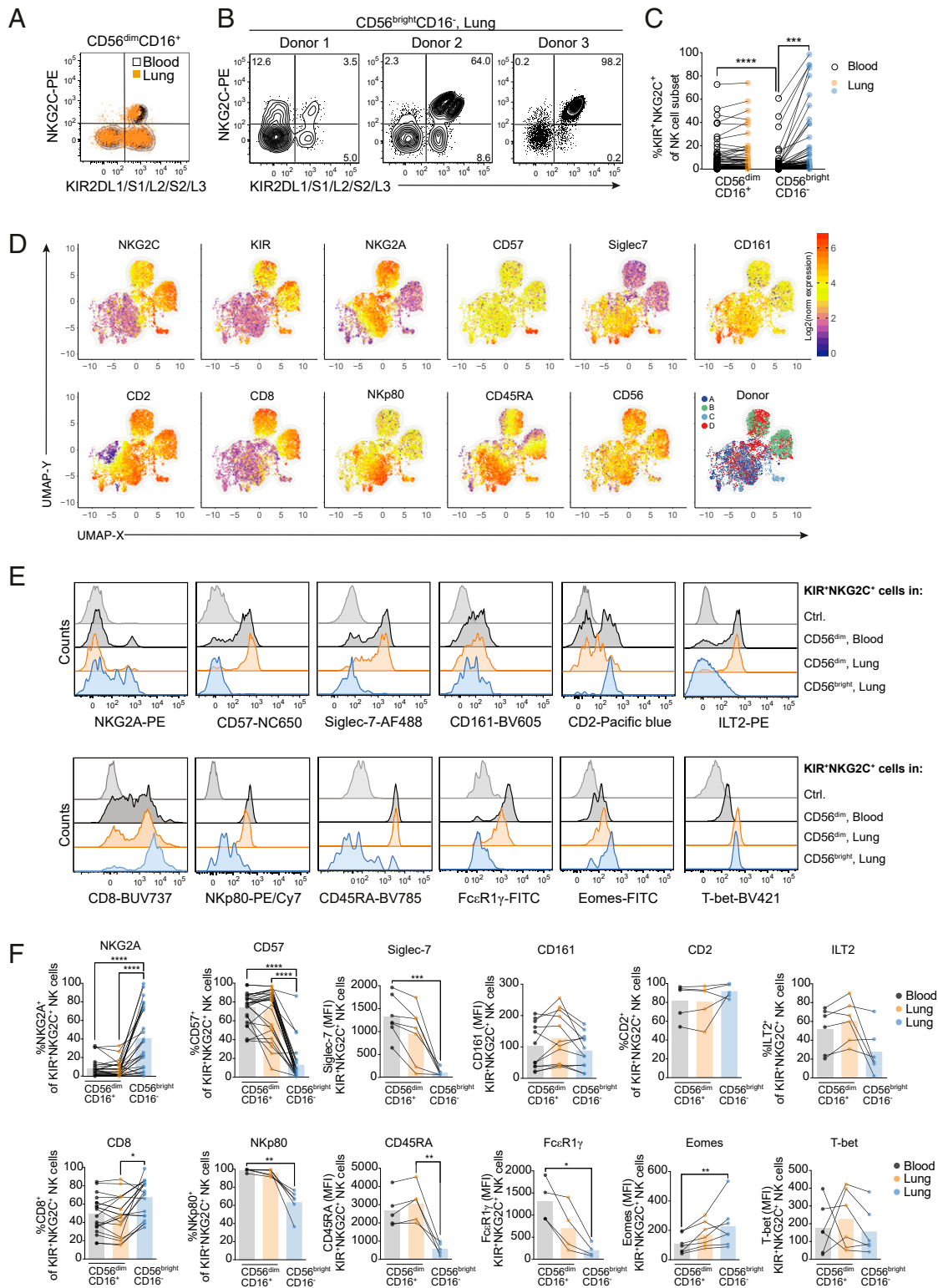
Fig. 1. Identification of adaptive-like KIR+NKG2C+CD56bright CD16− NK cells in human lung. (*A*) Representative overlay displaying pan-KIR and NKG2C expression on CD56dimCD16+ NK cells in paired blood (black contour) and lung (orange). (*B*) Representative dot plots displaying pan-KIR and NKG2C expression on CD56brightCD16− NK cells in the lungs of three different donors. (*C*) Frequencies of KIR+NKG2C+ NK cells in CD56dimCD16+ and CD56brightCD16− NK cells in paired blood and lung (n = 77). (*D*) UMAP analysis of CD56brightCD16− lung NK cells from four donors based on expression of Siglec-7, CD8, CD2, CD57, CD161, NKG2C, CD56, CD45RA, NKG2A, and NKp80. Color scale shows log2(normalized expression + 1). (*E*) Representative histograms and (*F*) summary of data showing surface expression of NKG2A (n = 27), CD57 (n = 27), Siglec-7 (n = 7), CD161 (n = 12), CD2 (n = 5), ILT2 (n = 6), CD8 (n = 20), NKp80 (n = 6), and CD45RA (n = 5) and intracellular expression of FcεR1γ (n = 4), Eomes (n = 7), and T-bet (n = 6) in KIR+NKG2C+ NK cells in CD56dimCD16+ blood (gray) and lung (orange) NK cells and CD56brightCD16− lung NK cells (blue). Friedman test, Dunn's multiple comparisons test: *P < 0.05, **P < 0.01, ***P < 0.001, and ****P < 0.0001.

Brownlie et al.
Expansions of adaptive-like NK cells with a tissue-resident phenotype in human lung and blood

PNAS | 3 of 12
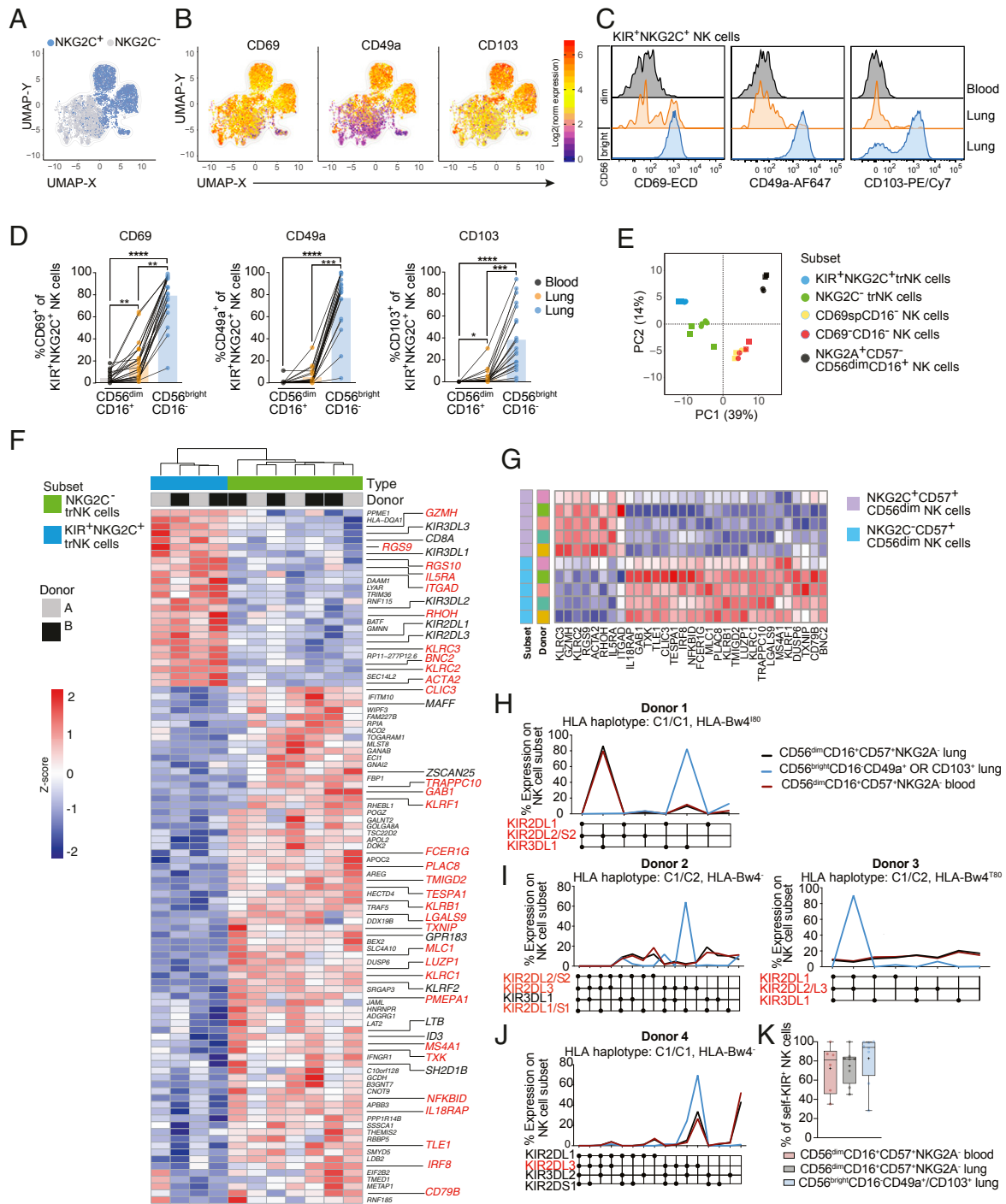https://doi.org/10.1073/pnas.2016580118

Fig. 2. Adaptive-like CD56^bright^CD16^−^ lung NK cells have a tissue-resident phenotype. (*A*) Overlay of UMAPs from data from Fig. 1 showing the position of NKG2C^+^ (blue) and NKG2C^−^ (gray) populations among CD56^bright^CD16^−^ NK cells. (*B*) Expression of the tissue-residency markers CD69, CD49a, and CD103 within the UMAP of CD56^bright^CD16^−^ lung NK cells. (*C*) Representative histograms and (*D*) summary of data showing the expression of CD69 (*n* = 23), CD49a (*n* = 21), and CD103 (*n* = 21) on CD56^dim^CD16^+^ blood (gray) and lung (orange) NK cells and CD56^bright^CD16^−^ lung NK cells (blue), respectively. Friedman test, Dunn's multiple comparisons test: **P* < 0.05, ***P* < 0.01, ****P* < 0.001, and *****P* < 0.0001. (*E*) PCA based on gene expression in the indicated subsets. (*F*) Heat map showing 102 DEGs between KIR^+^NKG2C^+^ trNK cells and KIR^−^NKG2C^−^ trNK cells in the human lung. DEGs shared with CD57^+^NKG2C^+^CD56^dim^CD16^+^ adaptive-like NK cells in blood (from GEO accession GSE117614) are highlighted in red. (*G*) Heat map showing gene expression in CD57^+^NKG2C^+^ and CD57^+^NKG2C^−^ CD56^dim^ NK cells for significant DEGs identified in comparisons of (NKG2C^−^) trNK cells vs. adaptive-like trNK cells in lung and in comparisons of CD57^+^NKG2C^−^ and CD57^+^NKG2C^+^ CD56^dim^ NK cells in blood. Data for CD56^dim^ pbNK cells are from GEO accession GSE117614 (22). (*H–J*) Single KIR expression analysis on donor-matched CD56^dim^CD16^+^CD57^+^NKG2A^−^ pbNK cells (red), CD56^dim^CD16^+^CD57^+^NKG2A^−^ (black), and CD56^bright^CD16^−^CD49a^+^/CD103^+^ (blue) lung NK cells from four donors. Self-KIRs are highlighted in red. (*H*) Donor with expansions of distinct self-KIR^+^ NK cells in CD56^dim^CD16^+^CD57^+^NKG2A^−^ NK cells and in CD56^bright^CD16^−^CD49a^+^/CD103^+^ lung NK cells. (*I*) Donors with an expansion of self-KIR^+^ NK cells exclusively in CD56^bright^CD16^−^CD49a^+^/CD103^+^ lung NK cells. (*J*) Donor with expansions of self-KIR^+^ NK cells both in CD56^dim^CD16^+^CD57^+^NKG2A^−^ NK cells and in CD56^bright^CD16^−^CD49a^+^/CD103^+^ lung NK cells. (*K*) Frequencies of self-KIR^+^ cells in indicated NK cell subsets in blood and lung (blood, *n* = 6; lung, *n* = 8). Box and whiskers indicate minimum to maximum. The plus sign indicates the mean.
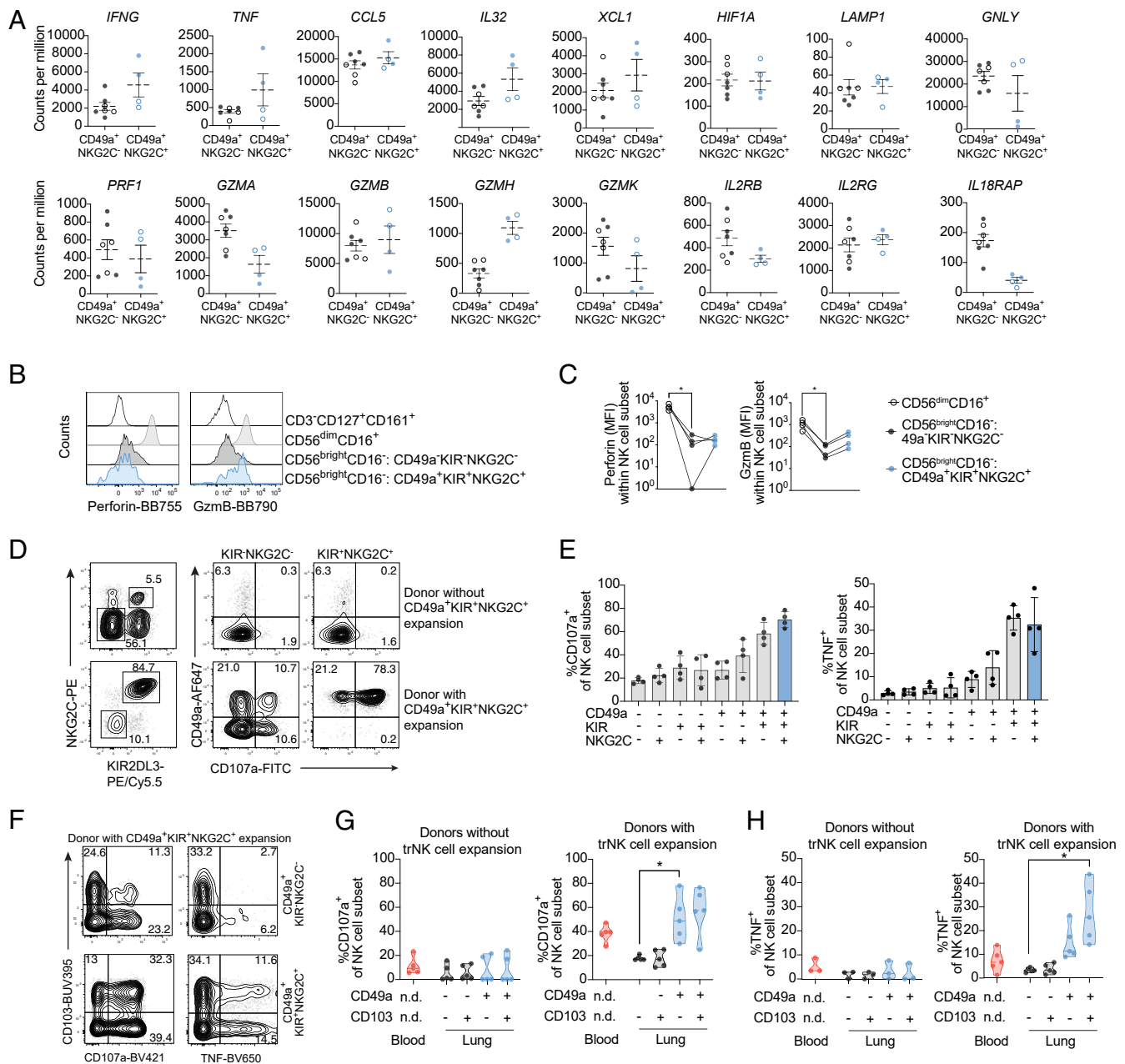
Fig. 3. Adaptive-like lung trNK cells are highly functional. (*A*) Gene expression levels (counts per million reads) for selected genes associated with functional capacity are shown for nonadaptive CD49a⁺KIR⁻NKG2C⁻ and adaptive-like CD49a⁺KIR⁺NKG2C⁺ lung trNK cells (clear circles, CD49a⁺CD103⁻ NK cells; filled circles, CD49a⁺CD103⁺ NK cells). Mean ± SEM is shown. (*B*) Representative histograms and (*C*) summary of data displaying ex vivo expression of perforin and granzyme B (GzmB; *n* = 4) in CD56^dim^CD16⁺, nonadaptive CD49a⁻CD56^bright^CD16⁻, and adaptive-like CD49a⁺CD56^bright^CD16⁻ lung NK cells. CD14⁻CD19⁻CD3⁻CD45⁺CD127⁺CD161⁺ cells were gated as controls in *B*. (*D*) Representative dot plots showing expression of CD107a and CD49a on KIR⁻NKG2C⁻ and KIR⁺NKG2C⁺ NK cells (*Left*) in a donor without (*Upper*) and with (*Lower*) expansion of adaptive-like trNK cells in the lung after stimulation with K562 cells. (*E*) Summary of data showing the frequency of K562 target cell-induced CD107a⁺ (*Left*) and TNF⁺ (*Right*) NK cell subsets from donors with NK cell expansions in the human lung. Responses by unstimulated controls were subtracted from stimulated cells (*n* = 4). Mean ± SD is shown. (*F*) Representative dot plots showing expression of CD107a and TNF vs. CD103 on nonadaptive CD49a⁺KIR⁻NKG2C⁻ (*Upper*) or adaptive-like CD49a⁺KIR⁺NKG2C⁺ (*Lower*) bulk NK cells in a donor with an expansion of adaptive-like trNK cells in the lung. (*G* and *H*) Summary of the frequencies of (*G*) CD107a⁺ and (*H*) TNF⁺ NK cells in pbNK cells and in subsets of lung NK cells (CD49a⁻CD103⁻, expressing either CD49a or CD103, or CD49a⁺CD103⁺) from donors without (*Left*, *n* = 5) or with (*Right*, *n* = 5) expansions of KIR⁺NKG2C⁺ trNK cells in the lung. Responses by unstimulated controls were subtracted from stimulated cells. (*G* and *H*) Violin plots with quartiles and median are shown. Friedman test, Dunn's multiple comparisons test. **P* < 0.05.

cells was independent of coexpression of CD103, since similar responses were observed between CD49a⁺CD103⁻ and CD49a⁺CD103⁺ KIR⁺NKG2C⁺ NK cells (Fig. 3 *F–H*). Furthermore, blood NK cells from donors with expanded adaptive-like CD49a⁺ NK cells also responded stronger to target cells as compared to donors without such expansions (Fig. 3 *F–H*). Taken together, the presence of expanded adaptive-like CD49a⁺ NK cells is linked to hyperresponsivity toward target cells, implicating a role of these cells in active immune regulation within the lung.

Brownlie et al.
Expansions of adaptive-like NK cells with a tissue-resident phenotype in human lung and blood

PNAS | 5 of 12
https://doi.org/10.1073/pnas.2016580118

Adaptive-Like CD49a$^+$ NK Cells Can Be Identified in Matched Patient Peripheral Blood. As a hallmark of tissue-resident cells, CD49a is commonly expressed on subsets of T cells and NK cells in nonlymphoid compartments such as the lung (14), liver (7), skin (24), uterus (25), and intestine (26), but not in peripheral blood. Intriguingly, however, we identified a small subset of CD49a^{+-}KIR$^+$NKG2C$^+$ NK cells within the CD16$^-$ NK cell population in paired peripheral blood of donors harboring expansions of adaptive-like CD49a$^+$ NK cells in the lung (Fig. 4 *A* and *B*; gating strategy is shown in *SI Appendix*, Fig. S1*E*). The frequencies of CD49a$^+$KIR$^+$NKG2C$^+$CD16$^-$ NK cells in peripheral blood (herein identified as CD49a$^+$ pbNK cells) were considerably lower compared to either adaptive-like CD49a$^+$ lung NK cells or adaptive-like CD56^{dim}CD16$^+$ pbNK cells, respectively (Fig. 4*B*). We observed that 18.6% and 25.6% of all donors had an expansion (identified as outliers) of adaptive-like CD49a$^+$ NK cells in lung and paired peripheral blood, respectively. In comparison, 20.9% and 15.1% of all donors had an expansion of adaptive-like CD56^{dim}CD16$^+$ pbNK cells in lung and paired blood, respectively (Fig. 4*B*). Interestingly, expansions of adaptive-like CD49a$^+$ and CD56^{dim}CD16$^+$ pbNK cells were virtually mutually exclusive in donors (Fig. 4*C*). However, there was a substantial overlap within each of these subsets between lung and peripheral blood (Fig. 4*C*), revealing a high likelihood of expansions of adaptive-like CD49a$^+$ NK cells both in lung and blood. Adaptive-like CD49a$^+$ pbNK cells expressed intermediate levels of CD57 with relatively low coexpression of NKG2A (Fig. 4 *D* and *E*), in contrast to lower expression of CD57 and higher expression of NKG2A in the adaptive-like CD49a$^+$ NK cells in lung (Fig. 1 *E* and *F*). Furthermore, adaptive-like CD49a$^+$ pbNK cells differed from their counterpart in lung by low expression of both CD69 and CD103 (Fig. 4 *D* and *E*), consistent with known phenotypic differences between tissue-resident and circulating lymphocyte populations (14, 27–29).

Taken together, adaptive-like CD49a$^+$ pbNK cells are linked to adaptive-like CD49a$^+$ NK cells in the human lung and are potentially emerging independently from adaptive-like CD56^{dim}CD16$^+$ pbNK cells.

Peripheral Blood Adaptive-Like CD49a$^+$ pbNK Cells from Healthy Donors Share Features with Adaptive-Like CD49a$^+$ Lung NK Cells and Adaptive-Like CD56^{dim}CD16$^+$ pbNK Cells. The presence of adaptive-like CD49a$^+$ NK cells in lungs of patients undergoing surgery for suspected lung cancer did not significantly correlate with any demographic or clinical parameters (*SI Appendix*, Fig. S4*A–F*). We next sought to determine if adaptive-like CD49a$^+$ NK cells could also be detected in the peripheral blood of unrelated healthy donors. Indeed, we found KIR$^+$NKG2C$^+$ NK cells coexpressing CD49a in the CD56^{bright}CD16$^-$ NK cell subset in 16% of healthy blood donors (Fig. 5 *A* and *B*). The frequencies of CD49a$^+$ pbNK cells among CD16$^-$ NK cells were lower in healthy peripheral blood (up to 5%, mean 0.3%) as compared to those found in patients with suspected lung cancer (up to 21%, mean 1.2%; Fig. 5*B*). Within the CD56^{bright}CD16$^-$ NK cell subset, KIR$^+$NKG2C$^+$ NK cells were almost exclusively detected in the CD49a$^+$ population (Fig. 5*C*). Similar to CD56^{bright}CD16$^-$CD49a$^+$ lung trNK cells (Fig. 2 *H–J*), the single-KIR expression pattern of CD56^{bright}CD16$^-$CD49a$^+$NKG2C$^+$ pbNK cells was distinct from the pattern in CD57$^+$NKG2A$^-$CD56^{dim}CD16$^+$ pbNK cells in some but not all donors (Fig. 5*D*). UMAP analysis of CD56^{bright}CD16$^-$ NK cells from healthy donors with CD49a$^+$ pbNK cells revealed a strong separation of the CD49a$^+$ NK cell subset coexpressing KIR and NKG2C based on lower expression or lack of CD69, CD38, NKp80, NKG2A, and TIM-3 as well as high expression of CD8, CXCR3, and granzyme B on CD49a$^+$KIR$^+$NKG2C$^+$ NK cells (Fig. 5*E*). This phenotype could be confirmed in individual samples (Fig. 5*F*). Interestingly, strong expression of CXCR6 could be identified on CD69$^+$ NK cells but not on adaptive-like CD49a$^+$
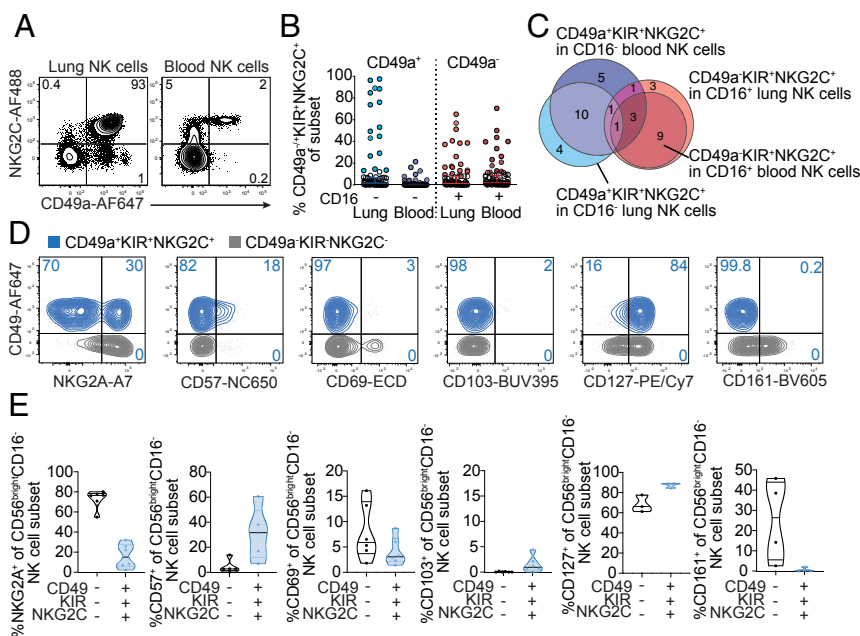

Fig. 4. Expansions of adaptive-like trNK cell in the lung is linked to presence of adaptive-like CD49a$^+$CD56^{bright}CD16$^-$ NK cells in paired blood. (*A*) Representative dot plots displaying expression of CD49a and NKG2C on NK cells in lung and paired peripheral blood. (*B*) Frequencies of adaptive-like CD49a$^+$ NK cells of CD16$^-$ trNK cells and of adaptive-like pbNK cells in the CD16$^+$ NK cell subset in paired lung and peripheral blood. Adaptive-like NK cell expansions were identified as outliers (filled circles) using the robust regression and outlier removal (ROUT) method (ROUT coefficient Q = 1). Median with interquartile range is shown (*n* = 86). (*C*) Euler diagram indicating overlaps and relationships between adaptive-like trNK and pbNK cell expansions in peripheral blood and lung. The number of individuals with overlaps between the subsets and compartments are indicated in the circles. (*D*) Representative overlays and (*E*) summary of data showing phenotypic differences between adaptive-like CD49a$^+$ (blue) and nonadaptive CD49a$^-$ (gray) CD56^{bright}CD16$^-$ pbNK cells (NKG2A, *n* = 6; CD57, *n* = 5; CD69, *n* = 6; CD103, *n* = 6; CD127, *n* = 3; CD161, *n* = 4). Violin plots with quartiles and median are shown.
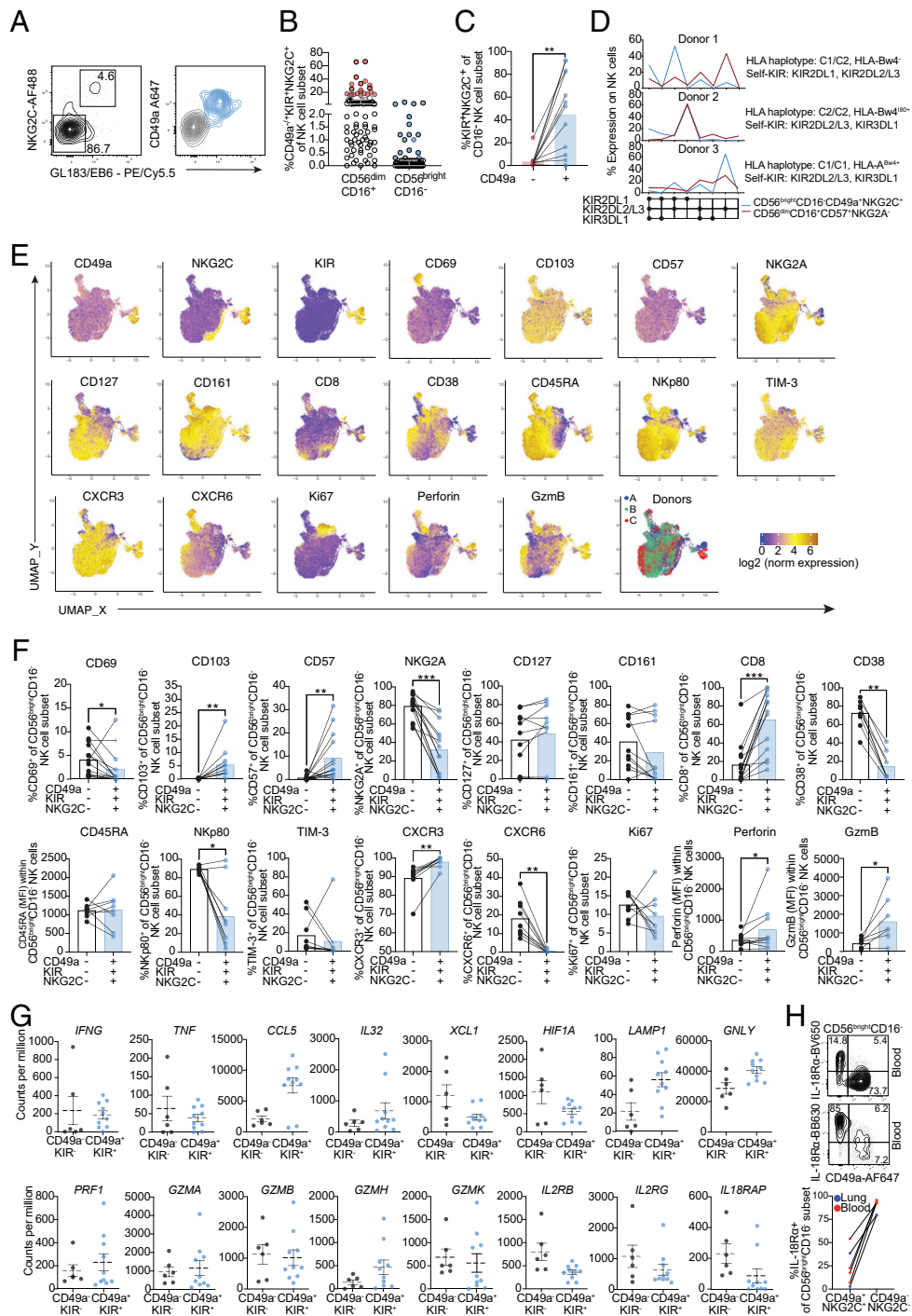
Fig. 5. Expansions of adaptive-like CD49a⁺CD56^bright^CD16⁻ NK cells in healthy blood donors. (*A*) Representative dot plot (*Left*) and overlay (*Right*) showing expression of KIR and NKG2C (*Left*) and CD49a on adaptive-like KIR⁺NKG2C⁺ NK cells (blue) vs. nonadaptive KIR⁻NKG2C⁻ NK cells (gray; *Right*) within CD16⁻ blood NK cells of healthy blood donors. (*B*) Identification of expansions (filled circles) of adaptive-like CD56^dim^CD16⁺ pbNK cells (21 outliers, 20%) and adaptive-like CD49a⁺CD56^bright^CD16⁻ pbNK cells (17 outliers, 16%) via the ROUT method (Fig. 4*E*). Error bars show the median with interquartile range ($n = 95$). (*C*) Frequencies of KIR⁺NKG2C⁺ cells of CD49a⁻CD16⁻ or CD49a⁺CD16⁻ NK cells in healthy blood. The respective maternal population comprised at least 45 cells ($n = 13$). Wilcoxon matched-pairs signed rank test: **$P < 0.005$. (*D*) Single KIR expression analysis on CD56^dim^CD16⁺CD57⁺NKG2A⁻ (red) and CD56^bright^CD16⁻CD49a⁺NKG2C⁺ (blue) NK cells in peripheral blood of three different healthy donors. (*E*) UMAPs showing CD56^bright^CD16⁻ NK cells from three donors with KIR⁺NKG2C⁺CD56^bright^CD16⁻ NK cells. UMAPs are based on expression of CXCR3, CD161, Ki67, NKG2C, CD103, TIGIT, perforin, granzyme B, NKG2A, CD16, CD56, CD49a, CD38, CD8, CXCR6, CD4, CD57, CD45RA, NKp80, CD69, GL183/EB6 (KIR), and CD127. Color scale indicates log2(normalized protein expression + 1) for each parameter. (*F*) Summary of protein expression on adaptive-like CD49a⁺ NK cells from peripheral blood from healthy donors (CD69, $n = 14$; CD103, $n = 11$; CD57, $n = 14$; NKG2A, $n = 14$; CD127, $n = 11$; CD161, $n = 11$; CD8, $n = 14$; CD38, $n = 9$; CD45RA, $n = 8$; NKp80, $n = 9$; TIM-3, $n = 9$; CXCR3, $n = 8$; CXCR6, $n = 8$; Ki67, $n = 9$; perforin, $n = 10$; granzyme B, $n = 9$). Before–after plots with bars indicating the mean. Wilcoxon matched-pairs signed rank test: *$P < 0.05$, **$P < 0.005$, and ***$P < 0.001$. (*G*) Gene expression levels (counts per million reads) for selected genes associated with functional capacity are shown for CD49a⁻KIR⁻ and CD49a⁺KIR⁺ blood CD56^bright^CD16⁻ NK cells. Mean ± SEM is shown. (*H*) Representative dot plots (*Top*) and summary of data (*Bottom*) for IL-18Rα expression on CD49a⁻NKG2C⁻ and CD49a⁺NKG2C⁺ CD56^bright^CD16⁻ NK cells in peripheral blood ($n = 4$) and lung ($n = 2$).

Brownlie et al.
Expansions of adaptive-like NK cells with a tissue-resident phenotype in human lung and blood

PNAS | 7 of 12
https://doi.org/10.1073/pnas.2016580118

pbNK cells, indicating that the latter NK cell subset depends on other chemokine receptors such as CXCR3 for tissue homing.

To gain further insight into the adaptive-like CD49a$^+$ pbNK cells, we compared them to nonadaptive CD49a$^-$ pbNK cells using RNA-seq (Figs. 5G and 6A; *SI Appendix*, Fig. S1C, shows the gating strategy). We next investigated whether gene expression differences in adaptive-like CD49a$^+$ pbNK cells indicated a different functional profile. Adaptive-like CD49a$^+$ pbNK cells expressed particularly higher levels of *CCL5*, *LAMP1*, *GZMH*, and *GNLY* and lower levels of *XCL1*, *HIF1A*, *IL2RB*, and *L18RAP* (Fig. 5G). Hence, adaptive-like CD49a$^+$ pbNK cells and adaptive-like CD49a$^+$ lung NK cells from different donors (Fig. 3A) shared a common gene expression pattern for some (*CCL5*, *GZMH*, *IL2RB*, and *IL18RAP*), but not all (i.e., *GNLY*), genes, indicating that they are functionally distinct from each other but also from their nonadaptive counterparts. Low expression of IL18Rα was confirmed at the protein level both in blood and lung CD49a$^+$ adaptive-like NK cells (Fig. 5H).

Next, we assessed how CD49a$^+$ pbNK cells related to other NK cell subsets in blood and lung at the transcriptome level. By PCA, CD49a$^+$ pbNK cells clearly separated from CD49a$^-$ CD56^{bright}CD16$^-$ NK cells and formed a cluster distinct from adaptive-like KIR$^+$NKG2C$^+$ lung trNK cells (Fig. 6A). This indicated that CD49a$^+$ pbNK cells are, to some extent, more similar to adaptive-like and nonadaptive lung trNK cells compared to CD49a$^-$CD56^{bright}CD16$^-$ pbNK cells and CD57$^-$ NKG2A$^+$CD56^{dim}CD16$^+$ lung NK cells. To further dissect differences in gene expression between adaptive-like CD49a$^+$ CD56^{bright}CD16$^-$ pbNK cells and nonadaptive CD56^{bright}CD16$^-$ NK cells in peripheral blood from healthy donors, we next analyzed DEGs between these subsets. A total of 351 genes were differentially expressed ($P_{adj} < 0.01$, log2FC > 1) and clearly segregated the subsets (Fig. 6B).

Since adaptive-like CD49a$^+$ pbNK cells resembled, to some extent, adaptive-like CD49a$^+$ NK cells in the lung, we next sought to identify similarities to nonadaptive and adaptive-like trNK cells also at transcriptome level. Indeed, a large number of shared DEGs could be identified between adaptive-like CD49a$^+$ pbNK cells (compared to CD49a$^-$KIR$^-$CD56^{bright}CD16$^-$ NK cells in peripheral blood) and in nonadaptive lung trNK cells (defined as CD69$^+$CD49a$^+$CD103$^+$NKG2A$^+$NKG2C$^-$CD16$^-$ NK cells; compared to non–tissue-resident CD69$^-$CD56^{bright}CD16$^-$ lung NK cells), including high expression of *ITGA1*, *ZNF683*, *PRDM1*, and *CCL5*, as well as lower expression of *SELL*, *GPR183*, *IL18R1*, and *IL18RAP* (Fig. 6C). All of these genes have also been shown to be differentially expressed in trNK cells in the bone marrow and/or CD8$^+$ tissue-resident memory T cells (T$_{RM}$ cells) in lung (27, 29). It should, however, be noted that other core genes associated with tissue-resident lymphocytes (e.g., *S1PR1*, *S1PR5*, *CXCR6*, *ITGAE*, *RGS1*, *KLF2*, *KLF3*, and *RIPOR2*) were not differentially expressed between adaptive-like CD49a$^+$ pbNK cells and nonadaptive CD49a$^-$CD56^{bright}CD16$^-$NK cells, indicating that they only partially have a tissue-resident phenotype.

Next, we determined whether adaptive-like CD49a$^+$ pbNK cells share a common gene signature with adaptive-like CD49a$^+$ lung NK cells and/or CD56^{dim}CD16$^+$ pbNK cells. Indeed, adaptive-like CD49a$^+$ pbNK cells shared DEGs with adaptive-like CD49a$^+$ NK cells in lung (Fig. 6D), as well as with adaptive-like NKG2C$^+$CD57$^+$ CD56^{dim}CD16$^+$ pbNK cells (8, 22), including increased expression of *KIRs*, *KLRC2*, *GZMH*, *ITGAD*, *IL32*, and *CD8A* and decreased expression of *KLRB1*, *FCER1G*, *IL18RAP*, and *IL2RB2* (Fig. 6D and *SI Appendix*, Fig. S5A). Despite the similarities, adaptive-like CD49a$^+$ pbNK cells were still clearly distinct from adaptive-like KIR$^+$NKG2C$^+$ trNK cells in lung at the transcriptome level, and, upon a direct comparison, we identified a large number of DEGs involved in tissue residency, including higher expression of *S1PR1*, *KLF3*, and

RAP1GAP2 and lower expression of *CD69*, *CXCR6*, and *RGS1*, in CD49a$^+$ pbNK cells (*SI Appendix*, Fig. S5B).

Taken together, adaptive-like CD49a$^+$ pbNK cells share traits with both nonadaptive lung trNK cells and adaptive-like CD49a$^+$ lung NK and CD56^{dim}CD16$^+$ pbNK cells but do not fully display a tissue-resident phenotype at the protein and gene expression level.

Discussion

Human adaptive-like NK cells have been described within the CD56^{dim}CD16$^+$ subset in peripheral blood (5, 6, 8, 10, 30) and the CD56^{bright}CD16$^-$ subset in liver (7). Here, we identified and characterized a yet unexplored and unique subset of adaptive-like CD49a$^+$KIR$^+$NKG2C$^+$CD56^{bright}CD16$^-$ NK cells in the human lung and peripheral blood. Adaptive-like CD49a$^+$ lung NK cells shared several phenotypic features with other adaptive-like NK cell subsets both in blood and/or liver, including high expression of CD49a (liver), CD69 (liver), and CD2 (blood) and lack of, or decreased, expression of CD57 (liver), CD45RA (liver), and perforin (liver), as well as low expression of FcεR1γ and Siglec-7 (blood) (5, 7–10, 18, 30, 31). However, adaptive-like CD49a$^+$ lung NK cells segregate from adaptive-like liver NK cells on the basis of high expression of Eomes and CD103, and from adaptive-like CD56^{dim}CD16$^+$ pbNK cells by lack or low expression of CD57 and a CD56^{bright}CD16$^-$ phenotype (7). Transcriptome analysis revealed shared core genes in adaptive-like CD49a$^+$ lung NK cells and adaptive-like CD56^{dim}CD16$^+$ and CD56^{bright}CD16$^-$ pbNK cells, underlining common features between all adaptive-like NK cell populations. Intriguingly, adaptive-like CD49a$^+$ lung NK cells were highly target cell-responsive, reflecting an overall hyperresponsiveness in donors with expansions of adaptive-like CD49a$^+$ NK cells in the lung. These findings indicate in vivo priming akin to what has been observed previously in human antigen-dependent (3, 32), antigen-independent, and cytokine-dependent (2, 33–35) NK cell recall responses. Although adaptive-like CD49a$^+$ NK cells in both blood and lung expressed lower levels of IL-18Rα compared to CD49a$^-$CD56^{bright}CD16$^-$ NK cells (Fig. 5H), indicating that they would respond weaker to IL-18 stimulation alone, it remains possible that they could still be primed for target cell responsiveness by, e.g., IL-18 and IL-12, as was recently shown for adaptive-like CD56^{dim}CD16$^+$ pbNK cells (36). In line with our results, this emphasizes a role of potential cytokine-mediated priming of adaptive-like CD49a$^+$ NK cells in the human lung.

Despite potential in vivo priming, the presence of adaptive-like CD49a$^+$ NK cells in the lung donors did not correlate with any clinical or demographic parameters. In fact, we could identify adaptive-like CD49a$^+$ NK cells also in the peripheral blood of healthy donors. These adaptive-like CD49a$^+$ pbNK cells shared a gene signature with trNK cells in the human lung, indicating tissue imprinting. These findings suggest reentry of adaptive-like CD49a$^+$ NK cells from tissue into circulation and, hence, potential seeding of tissues with adaptive-like CD49a$^+$ lung NK cells via peripheral blood. In mice, MCMV-specific CD8$^+$ T cells convert to CD103$^+$ T$_{RM}$ cells, with small numbers of new T$_{RM}$ cells deriving from the circulation (37), and memory inflation is required for retention of CD8$^+$ T$_{RM}$ cells in the lungs after intranasal vaccination with MCMV (38), indicating a dynamic retention of T$_{RM}$ cells by a persistent infection. It remains to be determined whether virus-dependent expansion and maintenance occur analogously in adaptive-like CD49a$^+$ NK cells in the lung. However, T$_{RM}$ cells and adaptive-like CD49a$^+$ NK cells likely differ in their recruitment to the lung, with T$_{RM}$ cells being dependent on CXCR6 (39), while adaptive-like CD49a$^+$ pbNK cells lack expression of CXCR6 but express CXCR3.

Adaptive-like CD49a$^+$ NK cell expansions were rarely observed in donors having adaptive-like CD56^{dim}CD16$^+$ pbNK cell
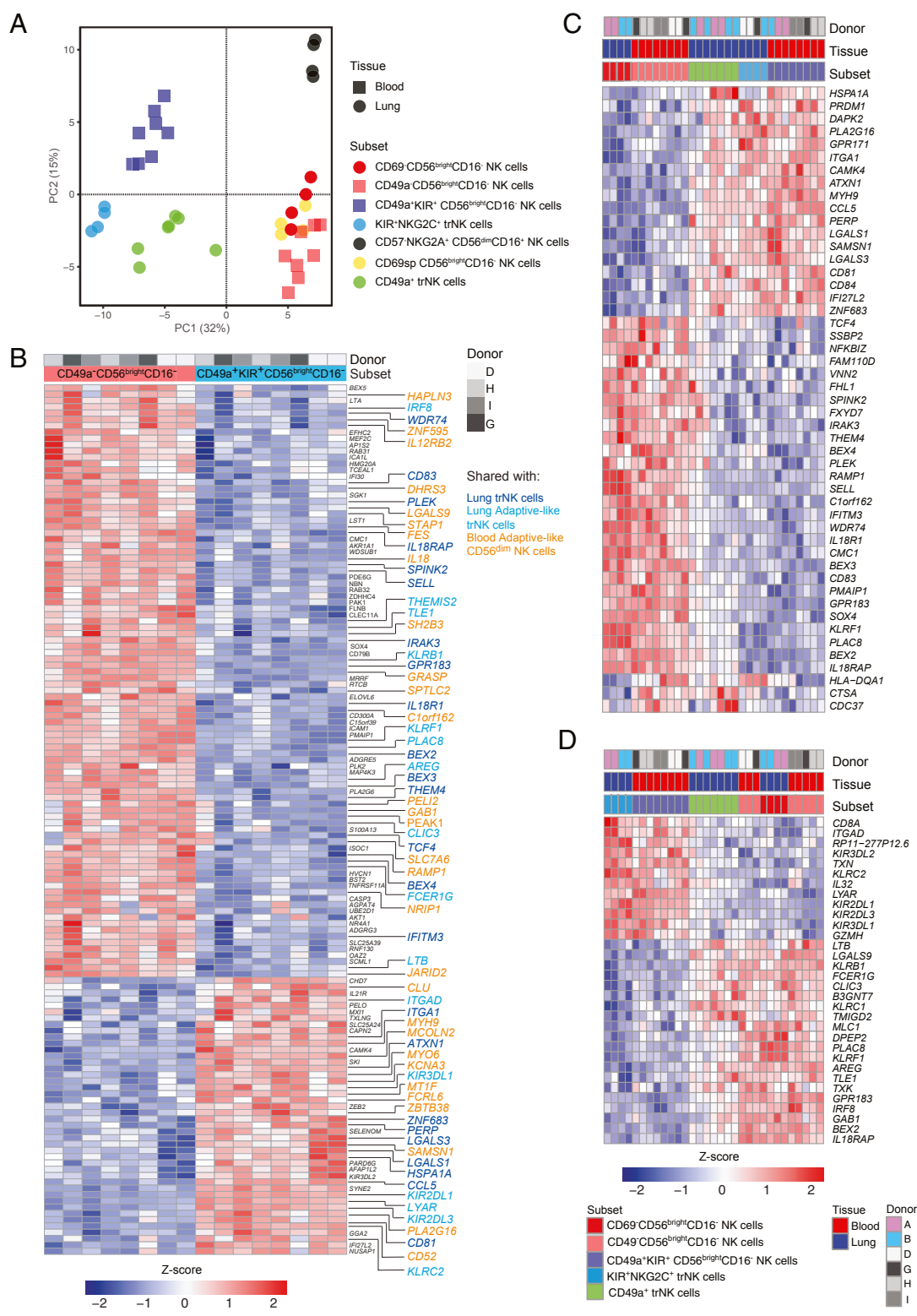
Fig. 6. Adaptive-like CD49a⁺CD56^bright^CD16⁻ pbNK cells in healthy blood donors share traits with both trNK cells and adaptive-like trNK cells. (*A*) PCA based on gene expression (1,000 most variable genes) in the indicated subsets in blood and lung. (*B*) Heat map showing 138 DEGs ($P_{adj} < 0.001$, log2FC > 2) between adaptive-like CD49a⁺CD56^bright^CD16⁻ NK cells and nonadaptive CD49a⁻CD56^bright^CD16⁻ NK cells in peripheral blood from healthy donors (*n* = 4). Genes shared with trNK cells in the lung are highlighted in dark blue, genes shared with adaptive-like trNK cells in bright blue, and genes shared with adaptive-like CD56^dim^CD16⁺ pbNK cells in orange. (*C* and *D*) Heat maps showing gene expression in CD69⁻CD56^bright^CD16⁻ lung NK cells, CD49a⁺ lung trNK cells, adaptive-like lung trNK cells, CD49a⁻CD56^bright^CD16⁻ pbNK cells, and CD49a⁺CD56^bright^CD16⁻ pbNK cells for (*C*) significant shared DEGs identified in CD49a⁺ pbNK cells (compared to CD49a⁻CD56^bright^CD16⁻ pbNK cells) and in CD49a⁺ lung trNK cells (compared to CD69⁻CD56^bright^CD16⁻ lung NK cells) and (*D*) in CD49a⁺ pbNK cells (compared to CD49a⁻CD56^bright^CD16⁻ pbNK cells) and in adaptive-like lung trNK cells (compared to non–adaptive-like lung trNK cells).

Brownlie et al.
Expansions of adaptive-like NK cells with a tissue-resident phenotype in human lung and blood

PNAS | 9 of 12
https://doi.org/10.1073/pnas.2016580118

expansions, indicating that these two distinct subsets have different developmental cues. Indeed, even in the rare cases where we could detect expansions of both adaptive-like CD49a^{+} NK and CD56^{dim}CD16^{+} pbNK cells in the same individual, these populations had distinct KIR repertoires. Furthermore, while expansions of adaptive-like CD56^{dim}CD16^{+} pbNK cells are restricted to HCMV-seropositive individuals (*SI Appendix*, Fig. S4E) (5, 30), expansions of adaptive-like CD49a^{+} lung NK cells could be detected in HCMV-seronegative individuals, although the vast majority were detected in HCMV-seropositive individuals (*SI Appendix*, Fig. S4 *E–H*). HCMV seronegativity was confirmed by repeated ELISAs (*SI Appendix*, Fig. S4E), CMVpp65 dextramer staining, as well as with T cell stimulation assays with CMV peptide pools (*SI Appendix*, Fig. S4 *G and H*). It thus remains possible that other viral infections than CMV could drive the expansion of adaptive-like CD49a^{+} NK cells, as has previously been suggested for the generation of cytokine-induced memory NK cells, e.g., after viral infections in humans (40), mice (4, 41–43), and rhesus macaques (44). Taken together, our data support a model where adaptive-like CD49a^{+} NK and CD56^{dim}CD16^{+} pbNK cells develop independently from each other, possibly due to distinct environmental requirements for their expansion.

We observed increased gene expression levels of *GZMH* in adaptive-like CD49a^{+} lung and blood NK cells, as well as of *CCL5* in both nonadaptive CD49a^{+} and adaptive-like CD49a^{+} lung NK cells, as compared to CD69^{−}CD56^{bright}CD16^{−} lung NK cells. *CCL5* was particularly highly expressed in adaptive-like CD49a^{+} pbNK cells. An antiviral activity has been proposed for granzyme H (45, 46), indicating potential functional relevance in viral infections. *CCL5* is predominantly produced by mouse Ly49H^{+} NK cells upon stimulation with MCMV-derived m157 protein (47). Furthermore, hyperresponsiveness of adaptive-like CD49a^{+} lung NK cells suggests that they could be clinically relevant, e.g., in respiratory viral infections and/or the defense against malignant tumor cells. Similarly, lung CD8^{+} T_{RM} cells have previously been shown to be able to control tumor growth and to correlate with increased survival in lung cancer patients (48). Adaptive-like CD49a^{+} NK cells might exceed their counterpart in peripheral blood in tissue homing and tumor infiltration based on their expression of tissue-specific and lung-homing receptors; hence, these cells could be harnessed for future treatment options of solid tumors.

Together, our data reveal the presence of a yet unexplored and distinct adaptive-like CD49a^{+} NK cell subset in the human lung and blood. The presence of adaptive-like CD49a^{+} NK cells in paired peripheral blood allows a noninvasive identification of donors with potential adaptive-like CD49a^{+} NK cell expansions in the lung. Finally, adaptive-like NK cells with tissue-resident features and excessive functional responsiveness in the human lung and blood could be an attractive source for tailored cancer immunotherapies, in particular for targeting solid tumors.

Materials and Methods

Lung Patients and Healthy Blood. A total of 103 patients undergoing lobectomy for suspected lung cancer were included in this study for collection of lung tissue and paired peripheral blood. None of the patients received preoperative chemotherapy and/or radiotherapy. Patients with records of strong immunosuppressive medication and/or hematological malignancy were excluded from the study. Clinical and demographic details are summarized in *SI Appendix*, Table S1. Furthermore, healthy blood was collected from regular, unrelated blood donors. The Regional Ethical Review Board in Stockholm approved the study (approval numbers 2006–299/31, 2010/181–31/2, and 2018/1819–31/1), and all donors gave informed written consent prior to collection of samples.

Processing of Tissue Specimens and Peripheral Blood. Lung tissue was processed as previously described (17). Briefly, a small part of macroscopically tumor-free human lung tissue from each patient was transferred into ice-

cold Krebs–Henseleit buffer and stored on ice for less than 18 h until further processing. The tissue was digested using collagenase II (0.25 mg/mL; Sigma-Aldrich) and DNase (0.2 mg/mL; Roche), filtered, and washed in complete RPMI medium 1640 (Thermo Scientific) supplemented with 10% fetal bovine serum (Thermo Scientific), 1 mM L-glutamine (Invitrogen), 100 U/mL penicillin, and 50 μg/mL streptomycin (R10 medium). Finally, mononuclear cells from the lung cell suspensions and peripheral blood were isolated by density gradient centrifugation (Lymphoprep).

RNA-Seq and RNA-Seq Data Analysis. RNA of sorted NK cell subsets from blood and lung were sequenced and analyzed as described previously (14). Briefly, RNA-seq was performed using a modified version of the SMART-Seq2 protocol (49). For analysis of lung adaptive-like NK cells, live NKG2C^{+}KIR^{+} CD3^{−}CD14^{−}CD19^{−}CD56^{+}CD16^{−} NK cells were sorted from two donors and were compared to previously published data on CD69^{+}CD49a^{+}CD103^{−} and CD69^{+}CD49a^{+}CD103^{+} NKG2A^{+}CD16^{−} trNK cells (GEO accession GSE130379) (14). For analysis of KIR^{+}CD49a^{+} CD56^{bright}CD16^{−} NK cells, we sorted KIR^{+}CD49a^{+} and KIR^{−}CD49a^{−} live CD14^{−}CD19^{−}CD3^{−}CD56^{bright}CD16^{−} NK cells from cryopreserved peripheral blood mononuclear cells from four donors. Duplicates of 100 cells from each population from two individual donors were sorted into 4.2 μL of lysis buffer (0.2% Triton X-100, 2.5 μM oligo-dT [5′-AAGCAGTGGTATCAACGCAGAGTACT30VN-3′], 2.5 mM dNTP, RNase Inhibitor [Takara], and ERCC RNA Spike-In Control [Ambion]) in a 96-well V-bottom PCR plate (Thermo Fisher). Sorted cells were then frozen and stored at −80 °C until they could be processed. Subsequent steps were performed following the standard SMART-Seq2 protocol with 22 cycles of complementary DNA (cDNA) amplification, and sample quality was determined using a bioanalyzer (Agilent High Sensitivity DNA chip). Five nanograms of amplified cDNA was taken for tagmentation using a customized in-house protocol (50) and Nextera XT primers. Pooled samples were sequenced on a HiSeq2500 device on high-output mode with paired 2 × 125-bp reads.

Transcriptome Analysis. Following sequencing and demultiplexing, read pairs were trimmed from Illumina adapters using cutadapt (version 1.14) (51), and UrQt was used to trim all bases with a phred quality score below 20 (52). Read pairs were subsequently aligned to the protein coding sequences of the human transcriptome (gencode.v26.pc_transcripts.fa) using Salmon (version 0.8.2) (53), and gene annotation was performed using gencode.v26.annotation.gtf. The RNA-seq count data has been deposited at GEO with accession number GSE166654. RNA-seq data for nonadaptive trNK cells have previously been published (GEO accession GSE130379). DeSeq2 (54) was used to analyze RNA-seq data in R studio version 1.20. Briefly, raw count values were used as input into deSeq2, and variance stabilizing transformation was used to transform data. Data were batch- and patient-corrected using Limma (55). A cutoff of >100 counts across the samples was used to filter out low-expressed genes. Genes with an adjusted P value <0.05 and a log2FC greater than 1 were considered as differentially expressed between paired samples unless otherwise stated. Similarly, previously published data sets on adaptive-like NKG2C^{+}CD57^{+}CD56^{dim}CD16^{+} NK cells and conventional NKG2C^{−}CD57^{+}CD56^{dim} NK cells (GEO accession GSE117614) (22) were analyzed using deSeq2 to identify DEGs. Heat maps of gene expression were generated using Pheatmap in R and show the gene normalized z-score for DEGs (as determined above in deSeq2) for all donors and replicates.

Flow Cytometry. Antibodies and clones used for phenotyping, intracellular staining, and cell sorting are listed in *SI Appendix*, Table S2. Secondary staining was performed with streptavidin Qdot 605 or Qdot 585 (both Invitrogen), anti-mouse IgM (II/41, eFluor 650NC; eBioscience), or streptavidin BB-630 or streptavidin-BV650 (BD Biosciences) and Live/Dead Aqua (Invitrogen). After surface staining, cells were fixed and permeabilized using a FoxP3/Transcription Factor staining kit (eBioscience) for subsequent intracellular staining. Purified NKG2C (no. 134591; R&D Systems) was biotinylated using a FluoReporter Mini-Biotin XX protein labeling kit (Life Technologies) and detected using streptavidin-Qdot 585, 605, or 655 (Invitrogen).

Samples were analyzed on a BD LSRFortessa equipped with four lasers (BD Biosciences) or a BD FACSymphony A5 equipped with five lasers (BD Biosciences), and data were analyzed using FlowJo version 9.5.2 and version 10.6.1 (Tree Star). UMAPs were constructed in FlowJo 10.6.1 using the UMAP plugin. UMAP coordinates and protein expression data were subsequently exported from FlowJo, and protein expression for each parameter was normalized to a value between 0 and 100. UMAP plots were made in R using ggplot, and color scale shows log2(normalized protein expression +1).

DNA Isolation and KIR/HLA-Ligand Genotyping. Genomic DNA was isolated using a DNeasy Blood & Tissue Kit (Qiagen) from 100 μL of whole blood. KIR genotyping and KIR ligand determination were performed using PCR/sequence-specific primer technology with a *KIR* typing kit and a *KIR HLA* ligand kit (both Olerup-SSP) according to the manufacturer's instructions.

CMV IgG ELISA. Concentrations of anti-CMV IgG relative to a standard curve and internal negative and positive control were determined by ELISA (Abcam) and read in a microplate spectrophotometer (Bio-Rad xMark) at 450 nm with a 620-nm reference wavelength.

NK Cell Activation Assay. Degranulation and TNF production of fresh blood and lung NK cells were assessed as previously described (17, 56). In brief, fresh lung and blood mononuclear cells were resuspended in R10 medium and rested for 15 to 18 h at 37 °C. Subsequently, the cells were cocultured in R10 medium alone or in presence of K562 cells for 2 h in the presence of anti-human CD107a (FITC or Brilliant Violet 421, H4A3; BD Biosciences).

CMV-T Cell Assays. For analysis of HCMV-specific T cells, mononuclear cells from lung or blood were either stained with HLA-A2/CMV pp65 or HLA-B7/CMV pp65 dextramers (Immudex) together with antibodies against CD3, CD8, and CD49a or stimulated with CMV peptide pools (IE-1 and pp65; JPT Technologies) and 20 U IL-2 per milliliter for 6 d and then restimulated for an additional 6 h with peptide in the presence of Brefeldin A to enable detection of TNF and IFN-γ production by flow cytometry. As controls, cells were either cultured in media with 20 U/mL IL-2 alone or together with EBV peptide pools (LMP1 and BZLF1; Miltenyi).

Statistics. GraphPad Prism 6 and 7 (GraphPad Software) were used for statistical analysis. For each analysis, measurements were taken from distinct samples. The statistical method used is indicated in each figure legend.

Data Availability. All study data are included in the article and/or supporting information.The RNA-seq count data has been deposited at GEO with accession number GSE166654.

1. J. C. Sun, J. N. Beilke, L. L. Lanier, Adaptive immune features of natural killer cells. *Nature* **457**, 557–561 (2009).
2. M. A. Cooper *et al.*, Cytokine-induced memory-like natural killer cells. *Proc. Natl. Acad. Sci. U.S.A.* **106**, 1915–1919 (2009).
3. J. G. O'Leary, M. Goodarzi, D. L. Drayton, U. H. von Andrian, T cell- and B cell-independent adaptive immunity mediated by natural killer cells. *Nat. Immunol.* **7**, 507–516 (2006).
4. S. Paust *et al.*, Critical role for the chemokine receptor CXCR6 in NK cell-mediated antigen-specific memory of haptens and viruses. *Nat. Immunol.* **11**, 1127–1135 (2010).
5. M. Gumá *et al.*, Imprint of human cytomegalovirus infection on the NK cell receptor repertoire. *Blood* **104**, 3664–3671 (2004).
6. S. Lopez-Vergès *et al.*, Expansion of a unique CD57+NKG2Chi natural killer cell subset during acute human cytomegalovirus infection. *Proc. Natl. Acad. Sci. U.S.A.* **108**, 14725–14732 (2011).
7. N. Marquardt *et al.*, Cutting edge: Identification and characterization of human intrahepatic CD49a+ NK cells. *J. Immunol.* **194**, 2467–2471 (2015).
8. H. Schlums *et al.*, Cytomegalovirus infection drives adaptive epigenetic diversification of NK cells with altered signaling and effector function. *Immunity* **42**, 443–456 (2015).
9. J. Lee *et al.*, Epigenetic modification and antibody-dependent expansion of memory-like NK cells in human cytomegalovirus-infected individuals. *Immunity* **42**, 431–442 (2015).
10. V. Béziat *et al.*, NK cell responses to cytomegalovirus infection lead to stable imprints in the human KIR repertoire and involve activating KIRs. *Blood* **121**, 2678–2688 (2013).
11. A. Cerwenka, L. L. Lanier, Natural killer cell memory in infection, inflammation and cancer. *Nat. Rev. Immunol.* **16**, 112–123 (2016).
12. T. W. Kuijpers *et al.*, Human NK cells can control CMV infection in the absence of T cells. *Blood* **112**, 914–915 (2008).
13. Z. Chen, Y. Yang, L. L. Liu, A. Lundqvist, Strategies to augment natural killer (NK) cell activity against solid tumors. *Cancers (Basel)* **11**, 1040 (2019).
14. N. Marquardt *et al.*, Unique transcriptional and protein-expression signature in human lung tissue-resident NK cells. *Nat. Commun.* **10**, 3841 (2019).
15. G. E. Cooper, K. Ostridge, S. I. Khakoo, T. M. A. Wilkinson, K. J. Staples, Human CD49a+ lung natural killer cell cytotoxicity in response to influenza A virus. *Front. Immunol.* **9**, 1671 (2018).
16. C. L. Gordon *et al.*, Tissue reservoirs of antiviral T cell immunity in persistent human CMV infection. *J. Exp. Med.* **214**, 651–667 (2017).
17. N. Marquardt *et al.*, Human lung natural killer cells are predominantly comprised of highly differentiated hypofunctional CD69−CD56dim cells. *J. Allergy Clin. Immunol.* **139**, 1321–1330.e4 (2017).
18. L. L. Liu *et al.*, Critical role of CD2 co-stimulation in adaptive natural killer cell responses revealed in NKG2C-deficient humans. *Cell Rep.* **15**, 1088–1099 (2016).
19. J. Emgård *et al.*, Oxysterol sensing through the receptor GPR183 promotes the lymphoid-tissue-inducing function of innate lymphoid cells and colonic inflammation. *Immunity* **48**, 120–132.e8 (2018).
20. N. M. Adams *et al.*, Transcription factor IRF8 orchestrates the adaptive natural killer cell response. *Immunity* **48**, 1172–1182.e6 (2018).
21. C. M. Lau *et al.*, Epigenetic control of innate and adaptive immune memory. *Nat. Immunol.* **19**, 963–972 (2018).
22. F. Cichocki *et al.*, ARID5B regulates metabolic programming in human adaptive NK cells. *J. Exp. Med.* **215**, 2379–2395 (2018).
23. B. Foley *et al.*, Cytomegalovirus reactivation after allogeneic transplantation promotes a lasting increase in educated NKG2C+ natural killer cells with potent function. *Blood* **119**, 2665–2674 (2012).
24. S. Cheuk *et al.*, CD49a expression defines tissue-resident CD8+ T cells poised for cytotoxic function in human skin. *Immunity* **46**, 287–300 (2017).
25. R. Vento-Tormo *et al.*, Single-cell reconstruction of the early maternal-fetal interface in humans. *Nature* **563**, 347–353 (2018).
26. D. Masopust *et al.*, Dynamic T cell migration program provides resident memory within intestinal epithelium. *J. Exp. Med.* **207**, 553–564 (2010).
27. B. V. Kumar *et al.*, Human tissue-resident memory T cells are defined by core transcriptional and functional signatures in lymphoid and mucosal sites. *Cell Rep.* **20**, 2921–2934 (2017).
28. D. K. Sojka *et al.*, Tissue-resident natural killer (NK) cells are cell lineages distinct from thymic and conventional splenic NK cells. *eLife* **3**, e01659 (2014).
29. J. E. Melsen *et al.*, Human bone marrow-resident natural killer cells have a unique transcriptional profile and resemble resident memory CD8+ T cells. *Front. Immunol.* **9**, 1829 (2018).
30. V. Béziat *et al.*, CMV drives clonal expansion of NKG2C+ NK cells expressing self-specific KIRs in chronic hepatitis patients. *Eur. J. Immunol.* **42**, 447–457 (2012).
31. Q. Hammer, T. Rückert, C. Romagnani, Natural killer cell specificity for viral infections. *Nat. Immunol.* **19**, 800–808 (2018).
32. R. Nikzad *et al.*, Human natural killer cells mediate adaptive immunity to viral antigens. *Sci. Immunol.* **4**, eaat8116 (2019).
33. R. Romee *et al.*, Cytokine activation induces human memory-like NK cells. *Blood* **120**, 4751–4760 (2012).
34. R. Romee, M. Rosario, M. M. Berrien-Elliott *et al*, Cytokine-induced memory-like natural killer cells exhibit enhanced responses against myeloid leukemia. *Sci. Transl. Med.* **8**, 357ra123 (2016).
35. J. Ni *et al.*, Adoptively transferred natural killer cells maintain long-term antitumor activity by epigenetic imprinting and CD4+ T cell help. *OncoImmunology* **5**, e1219009 (2016).
36. Q. Hammer, T. Rückert, J. Dunst, C. Romagnani, Adaptive natural killer cells integrate interleukin-18 during target-cell encounter. *Front. Immunol.* **8**, 1976 (2018).
37. C. J. Smith, S. Caldeira-Dantas, H. Turula, C. M. Snyder, Murine CMV infection induces the continuous production of mucosal resident T cells. *Cell Rep.* **13**, 1137–1148 (2015).
38. K. M. Morabito *et al.*, Memory inflation drives tissue-resident memory CD8+ T cell maintenance in the lung after intranasal vaccination with murine cytomegalovirus. *Front. Immunol.* **9**, 1861 (2018).
39. S. Takamura, S. Kato, C. Motozono *et al*, Interstitial-resident memory CD8+ T cells sustain frontline epithelial memory in the lung. *J. Exp. Med.* **216**, 2736–2747 (2019).
40. M. R. Goodier *et al.*, Influenza vaccination generates cytokine-induced memory-like NK cells: Impact of human cytomegalovirus infection. *J. Immunol.* **197**, 313–325 (2016).
41. T. Li *et al.*, Respiratory influenza virus infection induces memory-like liver NK cells in mice. *J. Immunol.* **198**, 1242–1252 (2017).
42. Y. Dou *et al.*, Influenza vaccine induces intracellular immune memory of human NK cells. *PLoS One* **10**, e0121258 (2015).

IMMUNOLOGY AND INFLAMMATION

Brownlie et al.
Expansions of adaptive-like NK cells with a tissue-resident phenotype in human lung and blood

PNAS | 11 of 12
https://doi.org/10.1073/pnas.2016580118

43. G. O. Gillard *et al.*, Thy1+ NK [corrected] cells from vaccinia virus-primed mice confer protection against vaccinia virus challenge in the absence of adaptive lymphocytes. *PLoS Pathog.* **7**, e1002141 (2011).

44. R. K. Reeves *et al.*, Antigen-specific NK cell memory in rhesus macaques. *Nat. Immunol.* **16**, 927–932 (2015).

45. H. Tang, C. Li, L. Wang, H. Zhang, Z. Fan, Granzyme H of cytotoxic lymphocytes is required for clearance of the hepatitis B virus through cleavage of the hepatitis B virus X protein. *J. Immunol.* **188**, 824–831 (2012).

46. F. Andrade, E. Fellows, D. E. Jenne, A. Rosen, C. S. Young, Granzyme H destroys the function of critical adenoviral proteins required for viral DNA replication and granzyme B inhibition. *EMBO J.* **26**, 2148–2157 (2007).

47. B. G. Dorner *et al.*, Coordinate expression of cytokines and chemokines by NK cells during murine cytomegalovirus infection. *J. Immunol.* **172**, 3119–3131 (2004).

48. M. Nizard *et al.*, Induction of resident memory T cells enhances the efficacy of cancer vaccine. *Nat. Commun.* **8**, 15221 (2017).

49. S. Picelli *et al.*, Full-length RNA-seq from single cells using Smart-seq2. *Nat. Protoc.* **9**, 171–181 (2014).

50. S. Picelli *et al.*, Tn5 transposase and tagmentation procedures for massively scaled sequencing projects. *Genome Res.* **24**, 2033–2040 (2014).

51. M. Martin, Cutadapt removes adapter sequences from high-throughput sequencing reads. *EMBnet. J.* **17**, 10 (2011).

52. L. Modolo, E. Lerat, UrQt: An efficient software for the unsupervised quality trimming of NGS data. *BMC Bioinformatics* **16**, 137 (2015).

53. R. Patro, G. Duggal, M. I. Love, R. A. Irizarry, C. Kingsford, Salmon provides fast and bias-aware quantification of transcript expression. *Nat. Methods* **14**, 417–419 (2017).

54. M. I. Love, W. Huber, S. Anders, Moderated estimation of fold change and dispersion for RNA-seq data with DESeq2. *Genome Biol.* **15**, 550 (2014).

55. S. S. Weigt *et al.*, Gene expression profiling of bronchoalveolar lavage cells preceding a clinical diagnosis of chronic lung allograft dysfunction. *PLoS One* **12**, e0169894 (2017).

56. M. Scharenberg *et al.*, Influenza A virus infection induces hyperresponsiveness in human lung tissue-resident and peripheral blood NK cells. *Front. Immunol.* **10**, 1116 (2019).